EAST EUROPEAN JOURNAL OF PHYSICS. 3. 391-396 (2026)
DOI:10.26565/2312-4334-2026-3-35 ISSN 2312-4334

EFFECTS OF ADSORPTION OF SUBMONOLAYER Cs COATINGS ON THE ELECTRONIC STRUCTURE AND PHYSICAL PROPERTIES OF NiO AND MoO_3

A.U. Xujaniyazova, D.A. Tashmukhamedova, B.E. Umirzakov, M.B. Yusupjonova*, Z.R. Saidakhmedova, Sh.K. Salieva
Tashkent State Technical University named after Islam Karimov, Tashkent, 100095, Republic of Uzbekistan
**Corresponding Author e-mail: maxsuna.yusupjonova@gmail.com*
Received April 30, 2026; revised June 25, 2026; accepted June 30, 2026

Using methods for measuring the dependence of the true secondary electron yield δ on the primary electron energy E_p, as well as Auger-electron and photoelectron spectroscopy, the effects of Cs deposition with thickness θ from 0.2 to 4 monolayers on the composition, valence-electron density of states, and energy-band parameters of NiO and MoO_3 films were studied. It is shown that at θ = 1 monolayer (ML), the largest decrease in the electron affinity χ, the largest increase in the secondary electron yield δ, and the photoelectron quantum yield Y occur. At the same time, the band gap width E_g and the positions of peaks in the valence-electron spectra remain practically unchanged. It was shown for the first time that, for NiO, at θ = 1 ML, the surface electron affinity χ approaches zero. It is found that at θ > 1 ML, changes in the composition, structure, emission, and optical properties of the Cs–NiO system begin to be influenced by the thickness of the Cs film.
Keywords: *Transition metal oxides; Cesium adsorption; Electron affinity; Secondary electron emission; Photoemission*

INTRODUCTION

Transition metal oxides such as NiO and MoO_3 attract considerable interest due to their numerous applications in various fields [1–6], including electrochemical energy storage and photoelectrochemical devices, catalysis and sensing, lithium-ion batteries, flame-retardant materials, optical devices, and other electrochemical applications.

NiO is a wide-band-gap p-type semiconductor with a band gap in the range of 3.6–4.0 eV, depending on the oxide preparation technique and the measurement method [7–9]. MoO_3 is an indirect-band-gap n-type semiconductor with a band gap ranging from 2.8 to 3.6 eV, depending on the phase state and structure (bulk material, film, or nanostructure), as well as on the measurement technique [10–12].

Nickel and molybdenum oxide nanostructures can be fabricated by various methods, including thermal evaporation [13, 14], solution combustion [15], hydrothermal synthesis [16, 17], co-precipitation [18], wet-chemical methods [19], sol-gel processing [20, 21], and pyrolysis [22, 23]. In recent years, low-energy ion implantation has been widely employed to control the composition, structure, and properties of materials of various types [24-35].

In Ref. [24], nanometer-scale MoO_3 films were fabricated on a Mo single-crystal surface by thermal oxidation and ion implantation. The dependence of the Mo surface coverage by MoO_3 cluster phases on ion dose was determined. Films with a thickness of approximately 100 Å were obtained by sequential implantation of ions with energies of 5, 3, and 1 keV. It was established that thermal oxidation forms homogeneous MoO_3 films with good stoichiometry and thicknesses ranging from 50-60 to 600-700 Å, whereas ion implantation yields films with thicknesses ranging from 25-30 to 100 Å.

In Ref. [28], it was shown that implantation of MoO_3 with Ba^+ ions leads to the formation of an ion-modified layer consisting of Mo–O, Mo–Ba–O, and Ba–O compounds. This results in a significant modification of the valence-band density of states, a reduction of the work function Φ to 2.7 eV, a decrease in the band gap E_g by approximately 1.5 times, and a 1.5-fold increase in the maximum secondary electron emission coefficient σm.

In the present work, the effect of Cs atom adsorption with a thickness θ ranging from 0.2 to 4 monolayers (ML) on the composition, electronic structure, emission, and optical properties of the wide-band-gap semiconductors MoO_3 and NiO is investigated for the first time.

EXPERIMENTAL TECHNIQUE

All technological treatments (thermal annealing, oxidation, and ion implantation) and investigations of composition, electronic structure, and physical properties were carried out in the same ultrahigh-vacuum (UHV) system.

The elemental and chemical composition of the nanofilms was determined by Auger electron spectroscopy (AES), while the electronic structure was studied using ultraviolet photoelectron spectroscopy (UPS). Depth profiles of impurity distribution were obtained by layer-by-layer Auger analysis by sputtering the sample surface with Ar^+ ions at 1 keV and an incidence angle of approximately 80° to the surface normal. The etching rate was approximately (3 ± 1) Å/min. The uncertainty in determining atomic concentrations was approximately 5–6 at.%.

Cite as: A.U. Xujaniyazova, D.A. Tashmukhamedova, B.E. Umirzakov, M.B. Yusupjonova, Z.R. Saidakhmedova, Sh.K. Salieva, East Eur. J. Phys. 3, 391 (2026), https://doi.org/10.26565/2312-4334-2026-3-35

The photoelectron quantum yield Y was measured at a photon energy of $h\nu \approx 10.8$ eV. The energy dependence of the secondary electron emission (SEE) coefficient σ was measured in the primary electron energy range E_p = 100-1500 eV. Optical measurements were performed using AGILENT Cary 5000 UV-Vis-NIR spectrophotometer.

EXPERIMENTAL RESULTS AND DISCUSSION

Figure 1 shows the dependence of the true secondary electron yield (TSE) δ on the primary electron energy Ep in the range 1–15 eV for NiO with Cs films of different thicknesses. It can be seen that at θ = 0, a sharp increase in δ begins at E_p = 5.21 eV, corresponding to the onset of electron emission from the top of the valence band, Ev, to the vacuum level, E_{vac}. At θ = 0.5 ML, a sharp increase in δ is observed starting from E_p = 4.3 eV; at θ = 1 ML from E_p = 3.6 eV; and at θ = 2 and 4 ML from E_p = 4.0 eV. At θ ≥ 1 ML, the value of δ at all E_p values is lower than that for pure NiO. This is due to the fact that at θ ≥ 1 ML, true secondary electrons originate not only from NiO but also from the Cs film.

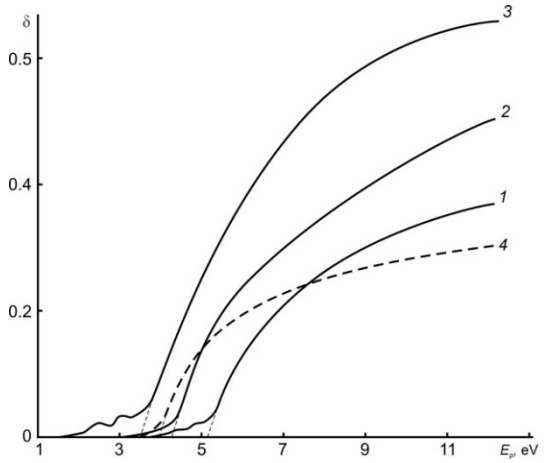

Figure 1. Dependences δ(E_p) in the range E_p = 1–15 eV for NiO with Cs films of thickness θ, ML: 1 – 0; 2 – 0.5; 3 – 1.0; 4 – 2

Since the emission efficiency of Cs is significantly lower than that of NiO starting from θ = 1 ML, the value of δ decreases over the entire E_p range as the thickness of the Cs film increases. In the initial part of the δ(E_p) dependence for NiO films, weak features associated with the presence of impurity levels are observed. With the shift of the spectrum's lower end toward lower E_p values during Cs adsorption, the positions of impurity levels also shift in parallel. It can be assumed that during Cs adsorption at θ ≤ 1 ML, the positions of the impurity levels remain unchanged. However, at θ > 1 ML, these impurity levels are poorly detected.

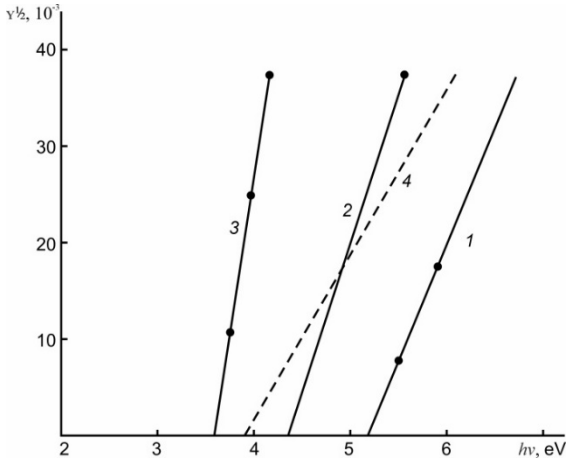

Figure 2. Dependences of $Y^{1/2}$ on $h\nu$ for NiO with Cs films of thickness θ, ML: 1 – 0; 2 – 0.5; 3 – 1.0; 4 – 4

At the same time, spectral distributions of the photoelectron quantum yield were recorded for the studied samples. Figure 2 shows Fowler plots (dependences of $Y^{1/2}$ on $h\nu$) for NiO with Cs films of different thicknesses. It can be seen that the photoelectron work function values at the top of the valence band (Ev) for NiO and NiO with Cs films of thicknesses 0.5, 1.0, and 2 ML are in good agreement with the data in Fig. 1.

Figure 3 shows the dependence of the light transmittance coefficient T on photon energy hν for pure NiO and NiO with Cs films of thickness θ = 0.5 and 1 ML. It is observed that the value of T remains nearly unchanged up to $h\nu$ = 3.5 eV, then decreases sharply to zero. Extrapolation of the second part of the curve to the $h\nu$ axis gives an approximate value of the band gap E_g. For NiO, E_g = 3.72 eV. After Cs deposition with thicknesses of 0.5 and 1 ML,

the value of T slightly decreases in the range *hv* from 7.0 to 3.2 eV, but the value of E_g remains practically unchanged. This shows that for Cs deposition with $\theta \leq 1$, the band gap E_g does not change significantly, and the decrease in the photoelectron work function Φ is mainly due to a decrease in the electron affinity χ.

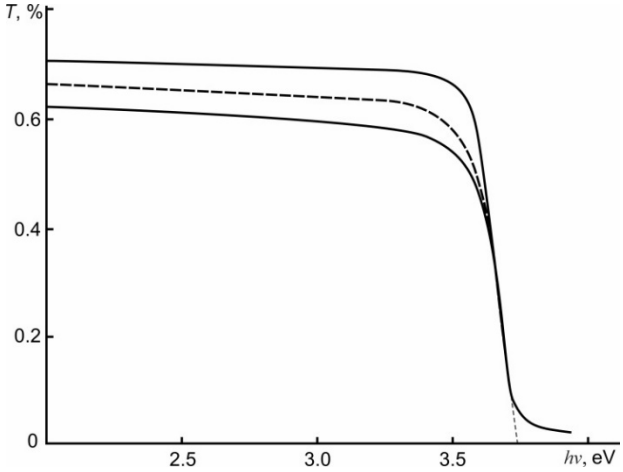

Figure 3. Dependences of the light transmittance coefficient T on photon energy *hv* for NiO with film thickness θ, ML: 1 – 0; 2 - 0.5; 3 – 1.0

Based on these data, we determined the work function Φ of NiO with a thin Cs film (Fig. 4). One monolayer was taken as the reference, corresponding to the minimum eφ value. From Fig. 4, it can be seen that during deposition for 1.2 min, the dependences Φ(t) and χ(t) pass through a minimum, decreasing by about ~ 2 eV. At t = 2.4 min, θ equals 2 monolayers; at t = 4.8 min, θ = 4 ML. At θ = 2 monolayers, the values of Φ and χ slightly increase and then remain practically unchanged with further increase in θ, i.e., the value of Φ characteristic of a thick Cs film is established.

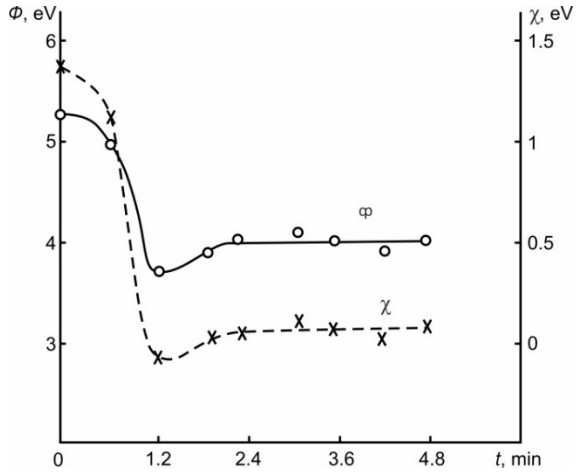

Figure 4. Dependence of the photoelectron work function Φ and electron affinity χ on the Cs deposition time on the NiO surface

Table 1 presents the energy-band parameters for NiO with Cs films of different thicknesses, determined from Figs. 1 and 3.

Table 1. Energy-band parameters and emission parameters for NiO with submonolayer Cs coverage

Parameters θ, ML	$\Phi = E_v$, eV	E_g, eV	χ, eV	σ_m	Y (at *hv* = 10.8 eV)
0	5.21	3.72	1.49	3.1	$6 \cdot 10^{-3}$
0.5	4.3	3.72	0.58	4.1	$9 \cdot 10^{-3}$
1	3.82	3.72	0.10	4.9	$3 \cdot 10^{-2}$
2	3.71	3.72	–0.01	3.9	$8 \cdot 10^{-3}$

From the table, it is evident that up to θ = 1 ML, as χ decreases, the values of Y and σ_m increase significantly. At θ = 1 ML, the value of χ approaches zero (Fig. 5).

Similar studies were also conducted on MoO_3 films. The results are summarized in Table 2. It can be seen that, in this case as well, Cs deposition does not change E_g, while Ev and χ decrease, and σ_m and Y increase noticeably. Unlike NiO, in the case of MoO_3, Cs adsorption with $\theta \leq 1$ leads to a much larger decrease in Φ and χ, but the effect of negative electron affinity does not occur.

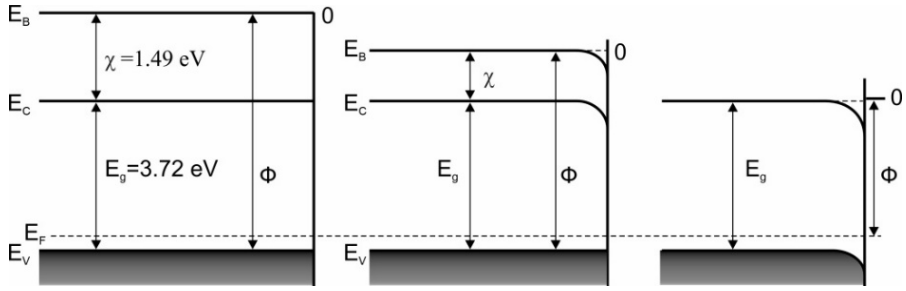

Figure 5. Energy diagrams of the surface: 1 – NiO; 2 – NiO with a Cs film of thickness 0.5 and 1 ML.

Table 2. Energy-band parameters and emission parameters of MoO_3 with submonolayer Cs coatings

$Cs^{\theta} \rightarrow MoO_3$	Parameters				
	E_v, eV	E_g, eV	χ, eV	σ_m	Y
θ = 0 ML	7.9	3.4	4.5	3.4	$4.5 \cdot 10^{-3}$
θ = 0.5 ML	6.2	3.4	2.8	–	-
θ = 1.0 ML	5.5	3.4	2.1	5.8	$6 \cdot 10^{-2}$
θ = 2.0 ML	5.7	3.4	2.3	4.5	$2 \cdot 10^{-2}$

"–" – measurements were not performed.

It should be noted that in the case of $Cs^{\theta} \rightarrow NiO$, at θ = 1 ML the value of χ approaches zero; however, a very sharp (10 times or more) increase in σm and Y, which is typical for semiconductors with negative electron affinity, is not observed. In addition, during Cs adsorption with θ = 1 ML for binary semiconductors (GaAs, GaP) and wide-band-gap semiconductors (MgO, WO_3), the value of χ decreases by 2.5 eV or more. In the case of NiO, this decrease is only about ~1.4 eV. These issues require further experimental and theoretical investigation.

CONCLUSIONS

1. For the first time, the influence of submonolayer Cs coatings on the electronic structure, emission, and optical properties of NiO and MoO_3 oxides has been investigated. It has been shown that at θ ≤ 1 monolayer, the values of σ_m and Y increase significantly, which is explained by a decrease in χ to 1.61 eV (NiO) and 2.4 eV (MoO_3).
2. It has been shown that during Cs adsorption at θ ≤ 1 ML, the composition of the surface layers remains practically unchanged; the band gap width and the valence-electron density-of-states structure also remain unchanged.
3. In the case of NiO, during Cs deposition at θ = 1 ML, a $Cs^{\theta} \rightarrow NiO$ system close to negative electron affinity is formed. However, in this case an increase in σ_m and Y is not observed.

ORCID

A.U. Xujaniyazova, https://orcid.org/0009-0003-3551-2831; **D.A. Tashmukhamedova,** https://orcid.org/0000-0001-5813-7518;
B.E. Umirzakov, https://orcid.org/0000-0002-9815-2111; **M.B. Yusupjonova,** https://orcid.org/0000-0003-1189-687X;
Z.R. Saidakhmedova, https://orcid.org/0009-0003-5363-7590; **Sh.K. Salieva,** https://orcid.org/0009-0004-4022-9309

REFERENCES

[1] T.U. Devi, E.R. Kumar, M. Kumar, B. Balraj, Ch. Sivakumar, P. Matheswaran, N. Chandrasekar, *et al*., "Physicochemical properties and photocatalytic activity of MoO_3 nanostructures: evaluation of structural, optical, vibrational, and morphological properties," Ceram. Int. **49**, 13994–14006 (2023). https://doi.org/10.1016/j.ceramint.2022.12.281
[2] D.K. Halwar, V.V. Deshmane, and A.V. Patil, "The combination of nickel oxide (NiO) and molybdenum trioxide (MoO_3) for pollutant gas detection," J. Electron. Mater. **52**, 1840–1853 (2023). https://doi.org/10.1007/s11664-022-10130-x
[3] N.G. Prakash, M. Dhananjaya, A.L. Narayana, D.P.M.D. Shaik, P. Rosaiah, and O.M. Hussain, "High-performance one-dimensional α-MoO_3 nanorods for supercapacitor applications," Ceram. Int. **44**, 9967–9975 (2018). https://doi.org/10.1016/j.ceramint.2018.03.032
[4] P.A. Dement'ev, E.V. Ivanova, M.N. Lapushkin, D.A. Smirnov, and S.N. Timoshnev, "Electronic structure of molybdenum oxidized in air," Phys. Solid State, **61**, 1993–1998 (2019). https://doi.org/10.1134/S1063783419110131
[5] F. Ma, Y. Zhao, J. Li, X. Zhang, H. Gu, and J. You, "Nickel oxide for inverted structure perovskite solar cells," J. Energy Chem. **52**, 393–411 (2021). https://doi.org/10.1016/j.jechem.2020.04.027
[6] M.M. Uplane, S.H. Mujawar, A.I. Inamdar, P.S. Shinde, A.C. Sonavane, and P.S. Patil, "Structural, optical, and electrochromic properties of nickel oxide thin films grown from electrodeposited nickel sulphide," Appl. Surf. Sci. **253**, 9365-9371 (2007). https://doi.org/10.1016/j.apsusc.2007.05.069
[7] H. Sato, T. Minami, S. Takata, and T. Yamada, "Transparent conducting p-type NiO thin films prepared by magnetron sputtering," Thin Solid Films, **236**, 27–31 (1993). https://doi.org/10.1016/0040-6090%2893%2990636-4
[8] M. Bonomo, "Synthesis and characterization of NiO nanostructures: A review," J. Nanopart. Res. **20**, 222 (2018). https://doi.org/10.1007/s11051-018-4327-y

[9] H.P. Parkhomenko, M.N. Solovan, and P.D. Maryanchuk, "Electrical properties of p-NiO/n-Si heterostructures based on nanostructured silicon," Semiconductors, **52**, 859–863 (2018). https://doi.org/10.1134/S1063782618070163
[10] M.B. Rammal, and S. Omanovic, "Synthesis and characterization of NiO, MoO_3, and $NiMoO_4$ nanostructures through a green facile method and their potential use as electrocatalysts for water splitting," Mater. Chem. Phys. **255**, 123570 (2020). https://doi.org/10.1016/j.matchemphys.2020.123570
[11] P.H. Silva, D.T. Cestarolli, and E.M. Guerra, "Band gap values and structural changes in MoO_3 obtained by ion-exchange method," Opt. Mater. 164, 117063 (2025). https://doi.org/10.1016/j.optmat.2025.117063
[12] E. Pavoni, M.G. Modreanu, E. Mohebbi, D. Mencarelli, P. Stipa, E. Laudadio, and L. Pierantoni, "First-principles calculation of MoO_2 and MoO_3 electronic and optical properties compared with experimental data," Nanomaterials, **13**, 1319 (2023). https://doi.org/10.3390/nano13081319
[13] A. Özkartal, and D.T. Noori, "Effects of thermal annealing on the characterization of p-NiO/n-GaAs heterojunctions produced by thermal evaporation," J. Mater. Sci.: Mater. Electron. **32**, 13462–13471 (2021). https://doi.org/10.1007/s10854-021-05924-4
[14] R. Senthilkumar, G. Anandhababu, T. Mahalingam, and G. Ravi, "Photoelectrochemical study of MoO_3 films with assorted morphologies formed by thermal evaporation," J. Energy Chem. **25**, 798–804 (2016). https://doi.org/10.1016/j.jechem.2016.04.005
[15] D. Parviz, M. Kazemeini, A.M. Rashidi, *et al*., "Synthesis and characterization of MoO_3 nanostructures by solution combustion method employing morphology and size control," J. Nanopart. Res. **12**, 1509–1521 (2010). https://doi.org/10.1007/s11051-009-9727-6
[16] B. Miao, W. Zeng, L. Lin, and Sh. Xu, "Characterization and gas-sensing properties of NiO nanowires prepared through the hydrothermal method," Physica E, **52**, 40–45 (2013). https://doi.org/10.1016/j.physe.2013.03.006
[17] J.-K. Song, J.-S. Ahn, and E.-M. Han, "Characteristics of perovskite solar cells with a nanostructured MoO_3 hole transport layer prepared by hydrothermal synthesis," Korean J. Mater. Res. **30**, 81–86 (2020). https://doi.org/10.3740/MRSK.2020.30.2.81
[18] M.Ch. Fite, S.D. Karse, and L.M. Gode, "Optical and photocatalytic properties of nickel oxide nanoparticles," J. Cryst. Growth, **660**, 128163 (2025). https://doi.org/10.1016/j.jcrysgro.2025.128163
[19] P.M. Ponnusamy, S. Agilan, N. Muthukumarasamy, T.S. Senthil, G. Rajesh, M.R. Venkatraman, and D. Velauthapillai, "Structural, optical, and magnetic properties of undoped NiO and Fe-doped NiO nanoparticles synthesized by a wet chemical process," Mater. Charact. **114**, 166–171 (2016). https://doi.org/10.1016/j.matchar.2016.02.020
[20] S. Kakherskyi, R. Pshenychnyi, O. Dobrozhan, *et al*., "Structural, microstructural, chemical, and optical properties of NiO nanocrystals and films obtained by 3D printing," Appl. Phys. A, **127**, 715 (2021). https://doi.org/10.1007/s00339-021-04847-5
[21] B.G. Bharate, "Synthesis of molybdenum oxide nanoparticles by the sol–gel method for ammonia gas sensing," Biomed. J. Sci. Tech. Res. **37**, 29172–29175 (2021). https://doi.org/10.26717/BJSTR.2021. 37.005957
[22] N. Mebrouki, S.B. Hamida, L. Benmebrouk, R. Gheriani, and L. Zenkhri, "Synthesis and characterization of nickel oxide thin films by spray pyrolysis: effect of nickel source nature," Asian J. Res. Chem. **15**, 159–162 (2022). https://doi.org/10.52711/0974-4150.2022.00026
[23] F. Chandoul, A. Boukhachem, F. Hosni, H. Moussa, M.S. Fayache, M. Amlouk, and R. Schneider, "Change in the properties of nanostructured MoO_3 thin films under gamma-ray irradiation," Ceram. Int. **44**, 12483–12490 (2018). https://doi.org/10.1016/j.ceramint.2018.04.040
[24] G.X. Allayarova, D.A. Tashmukhamedova, R. Djabbarganov, and B.E. Umirzakov, "Formation of nanoscale MoO_3 films by thermal oxidation and ion bombardment," J. Surf. Investig. **15**, 81–84 (2021). https://doi.org/10.1134/S1027451021010043
[25] S. Boulila, M. Ghamnia, A. Boukhachem, *et al*., "Photocatalytical properties of Ba-doped NiO nanofilms," Philos. Mag. Lett. **100**, 283–293 (2020). https://doi.org/10.1080/09500839.2020.1760389
[26] D.A. Tashmukhamedova, and M.B. Yusupjanova, Journal of Surface Investigation: X-ray, Synchrotron and Neutron Techniques. **15**(5), 1054-1057 (2021). https://doi.org/10.1134/S1027451021050402
[27] Y. Aoun, M. Marrakchi, S. Benramache, *et al*., "Preparation and characterization of monocrystalline Na-doped NiO thin films," Mater. Res. **21**, e20170681 (2018). https://doi.org/10.1590/1980-5373-mr-2017-0681
[28] B.E. Umirzakov, D.A. Tashmukhamedova, S.T. Gulyamova, *et al*., Effect of Ba^+ ion implantation on the composition and electronic properties of MoO_3/Mo(111) films," Tech. Phys. **65**, 795–798 (2020). https://doi.org/10.1134/S1063784220050242
[29] D.A. Tashmukhamedova, M.B. Yusupjanova, G.Kh. Allayarova, and B.E. Umirzakov, "Crystal structure and band gap of nanoscale phases of Si formed at various depths of the near-surface region of SiO_2," Technical Physics Letters, **46**(10), 972-975 (2020). https://doi.org/10.1134/S1063785020100144
[30] Sh. Wang, and A.J.R. Hensley, "Dopant effects on the environment-dependent chemical properties of NiO(100) surfaces," Appl. Surf. Sci. **682**, 161679 (2025). https://doi.org/10.1016/j.apsusc.2024.161679
[31] Kh.Kh. Boltaev, D.A. Tashmukhamedova, and B.E. Umirzakov, "Structure and electronic properties of nanoscale phases and nanofilms of metal silicides produced by ion implantation in combination with annealing," Journal of Surface Investigation, X_ray, Synchrotron and Neutron Techniques, **8**(2), 326–331 (2014). https://doi.org/10.1134/S1027451014010108
[32] Y.S. Ergashov, D.A. Tashmukhamedova, F.G. Djurabekova, and B.E. Umirzakov, "Effect of surface microroughness on the composition and electronic properties of CdTe/Mo(111) films," Bulletin of the Russian Academy of Sciences: Physics, **80**(2), 138 (2016). https://doi.org/10.3103/S1062873816020064
[33] B. E. Umirzakov, D. A. Tashmukhamedova, M. K. Ruzibaeva, *et al*., "Investigation of change of the composition and structure of the CaF_2/Si films surface at the low-energy bombardment," Nucl. Instr. and Meth. B. **326**, 322–325 (2014). https://doi.org/10.1016/j.nimb.2013.10.094
[34] D.A. Tashmukhamedova, "Study of composition and electronic structure of $CoSi_2$/Si interface" Bulletin of the Russian Academy of Sciences: Physics **70**(8), 1409-1411. (2006). https://elibrary.ru/item.asp?id=27854241
[35] M.B. Yusupjonova, D.A. Tashmukhamedova, B.E. Umirzakov, S.S. Pak, Z.R. Saidakhmedova, and Sh.K. Salieva, "Influence of implantation of active metal ions on the composition, emission and optical properties of MgO films," East European Journal of Physics, (1), 260-264 (2025). https://doi.org/10.26565/2312-4334-2025-1-29

ВПЛИВ АДСОРБЦІЇ СУБМОНОШАРОВИХ ПОКРИТТІВ Cs НА ЕЛЕКТРОННУ СТРУКТУРУ ТА ФІЗИЧНІ ВЛАСТИВОСТІ NiO ТА MoO_3

А.У. Хужаніязова, Д.А. Ташмухамедова, В.Е. Умірзаков, М.В. Юсупжонова, З.Р. Саїдахмедова, Ш.К. Солієва
Ташкентський державний технічний університет імені Іслама Карімова, Ташкент, 100095 Республіка Узбекистан

За допомогою методів вимірювання залежності справжнього виходу вторинних електронів δ від енергії первинних електронів E_p, а також спектроскопії Оже-електронів та фотоелектронів, досліджено вплив осадження Cs товщиною θ від 0,2 до 4 моношарів на склад, щільність станів валентних електронів та параметри енергетичних зон плівок NiO та MoO_3. Показано, що при θ = 1 ML відбувається найбільше зменшення електронної спорідненості χ та найбільше збільшення виходу вторинних електронів δ і квантового виходу фотоелектронів Y. При цьому ширина забороненої зони E_g та положення піків у спектрах валентних електронів практично не змінюються. Вперше показано, що для NiO при θ = 1 ML значення поверхневої електронної спорідненості χ наближається до нуля. Встановлено, що за θ > 1 ML зміни складу, структури, емісійних та оптичних властивостей системи Cs–NiO починають залежати від товщини плівки Cs.

Ключові слова: *оксиди перехідних металів; адсорбція цезію; електронна спорідненість; емісія вторинних електронів; фотоемісія*